

Uniaxial-stress tuned large magnetic-shape-memory effect in Ni-Co-Mn-Sb Heusler alloys

C. Salazar Mejía,^{1,a)} R. Kuchler,^{1,2} A. K. Nayak,^{1,3} C. Felser,¹ and M. Nicklas^{1,b)}

¹Max Planck Institute for Chemical Physics of Solids, Nöthnitzer Str. 40, 01187 Dresden, Germany

²Experimental Physics VI, Center for Electronic Correlations and Magnetism, University of Augsburg, Universitätsstr. 2, 86135 Augsburg, Germany

³Max Planck Institute of Microstructure Physics, Weinberg 2, 06120 Halle, Germany

(Received 9 December 2016; accepted 31 January 2017; published online 14 February 2017)

Combined strain and magnetization measurements on the Heusler shape-memory alloys $\text{Ni}_{45}\text{Co}_5\text{Mn}_{38}\text{Sb}_{12}$ and $\text{Ni}_{44}\text{Co}_6\text{Mn}_{38}\text{Sb}_{12}$ give evidence for strong magneto-structural coupling. The sample length changes up to 1% at the martensitic transformation, between a ferromagnetic, austenitic phase at high temperatures and a weakly magnetic, low-symmetry martensitic phase at lower temperatures. Under moderate uniaxial stress, the change in the sample length increases to and saturates at about 3%, pointing to stabilization of a single martensitic variant. A reverse martensitic transformation can also be induced by applying magnetic field: we find that within the temperature range of thermal hysteresis of the martensitic transformation, applying a field can induce a metastable expansion of the sample, while at slightly lower temperatures, the field response is reversible. These findings provide key information for future use of Ni(Co)-Mn-Sb-based Heusler compounds in, e.g., actuators and mechanical switches. *Published by AIP Publishing.*

[<http://dx.doi.org/10.1063/1.4976212>]

Magnetic shape memory (MSM) alloys have attracted a large amount of attention in the recent years.¹ The diverse potential applications of their non-magnetic counterparts are extended in the MSM alloys since the magnetic field can be used to control the shape-memory effect. Applications as sensors, actuators, and energy harvesters among others are in the focus of current research.^{2–4} Ni-Mn-based Heusler alloys are known to exhibit a MSM effect. In Ni-Mn-Ga alloys, MSM effects up to a field-induced change in the sample length of 12% have been reported,⁵ which originate from the re-orientation of variants in the martensitic state.^{7,8} In the Ni-Mn-Z series, where Z can be Sb, Sn, or In, the MSM effect has its origin in a magnetic-field-induced martensitic transformation (MT), which is connected to a metamagnetic transition.^{8–13} Values up to about 1% change in the sample length have been observed in polycrystalline Ni-Co-Mn-Sn.⁶ Superelasticity (or two-way MSM effect) has been reported for Ni-Mn-In alloys.¹⁴ In the case of the magnetic-field-induced MT, the change in the shape of the material arises from the difference in the volume of the austenitic and martensitic phases, being that the martensitic phase possesses a smaller volume than the austenitic phase. Additionally, the difference in the volume between the austenitic and martensitic phases makes these materials sensitive to application of external pressure. Pressure stabilizes the martensitic phase, and therefore, the MT shifts to higher temperatures.¹⁵ Furthermore, it has been reported that already small pressures can improve the magnetocaloric effect¹⁶ or lead to large barocaloric¹⁷ or elastocaloric effects.^{18–20} The combination of pressure and magnetic field tuning offers further possibilities

due to the fact that both act opposite on the MT, i.e., pressure favors the martensitic while the magnetic field stabilizes the austenitic phase.^{16,21–23}

The series of $\text{Ni}_{50-x}\text{Co}_x\text{Mn}_{38}\text{Sb}_{12}$ Heusler alloys has been widely studied.^{24–33} Depending on the Ni and Co composition, the materials exhibit a ferromagnetic transition in the high-temperature cubic austenitic phase followed by a MT at lower temperatures that drives the system to a weakly magnetic low-symmetry orthorhombic structure. With increasing Co content, the MT temperature decreases while the Curie temperature increases.²⁷ Ni-Co-Mn-Sb Heusler alloys have been shown to exhibit, among other phenomena, exchange bias,²⁶ giant magnetocaloric effect at room temperature,^{25,27} pressure-tuned MT,²⁴ reentrant spin-glass behavior,³⁰ kinetic arrest,²⁹ and elastocaloric effect.³³

In this work, we have studied the magnetostructural properties of two alloys from the series $\text{Ni}_{50-x}\text{Co}_x\text{Mn}_{38}\text{Sb}_{12}$ with the Co concentrations, $x = 5$ and 6, by strain, i.e., the relative change in the sample length, and magnetization experiments. We found length changes of more than 1% at the temperature and magnetic field induced MT. Within the MT hysteresis region, small changes in temperature have strong consequences on the observed properties. They can lead to either reversible or irreversible behaviors in the field dependence of strain and magnetization. In particular, a metastable length change can be induced by magnetic field in a narrow temperature region and canceled again by a small change in temperature. Furthermore, the length change at the MT can be strongly enhanced and optimized by the application of moderate uniaxial stress.

Polycrystalline ingots of $\text{Ni}_{50-x}\text{Co}_x\text{Mn}_{38}\text{Sb}_{12}$, $x = 5$ and 6, were prepared following Ref. 27. XRD data confirm a single cubic austenitic phase at room temperature as previously reported.^{26,30} Magnetization measurements were performed

^{a)}Present Address: Dresden High Magnetic Field Laboratory (HLD-EMFL), Helmholtz-Zentrum Dresden-Rossendorf, 01328 Dresden, Germany. Electronic mail: c.salazar-mejia@hzdr.de.

^{b)}Electronic mail: nicklas@cpfs.mpg.de.

in an MPMS3 (Quantum Design). A miniaturized high-resolution capacitance dilatometer was used to carry out temperature and magnetic field dependent strain measurements.³⁴ The experiments were conducted in a PPMS (Quantum Design) equipped with a 7 T superconducting magnet. The change in the length was recorded parallel to the direction of the magnetic field. In addition, strain was measured under uniaxial stress in an exchange-gas cryostat.³⁵ Samples of 1 to 2 mm length were used in the strain experiments.

The temperature dependence of the magnetization $M(T)$ and strain, expressed as the relative change in the sample length $\Delta L(T)/L_0 = [L(T) - L_0]/L_0$ (L_0 is the length of the sample at room temperature), for $\text{Ni}_{45}\text{Co}_5\text{Mn}_{38}\text{Sb}_{12}$ and $\text{Ni}_{44}\text{Co}_6\text{Mn}_{38}\text{Sb}_{12}$ are presented in Fig. 1. The MT is clearly visible as a step-like feature in both physical properties. Table I summarizes the characteristic temperatures of the MT extracted from our data.

We will first briefly discuss the magnetic properties of our samples before we turn to the results of the strain experiments. At the MT, upon cooling, $\text{Ni}_{45}\text{Co}_5\text{Mn}_{38}\text{Sb}_{12}$ exhibits an abrupt change from a large magnetization in the ferromagnetic austenitic phase to a small magnetization in the martensitic phase (see Fig. 1(a)). The MT is completely reversible with a thermal hysteresis of about 10 K. Application of a magnetic field leads to an almost linear shift of the MT toward lower temperatures by -1.7 K/T. This is a rather weak field dependence compared with other Heusler alloys.³⁶ Upon increasing field, the magnetization in both austenitic and martensitic phases increases considerably and, more remarkably, the size of the step in magnetization at the MT is strongly enhanced. A similar behavior is observed for $\text{Ni}_{44}\text{Co}_6\text{Mn}_{38}\text{Sb}_{12}$ as displayed in Fig. 1(c). The response of the MT to a magnetic field is slightly stronger in $\text{Ni}_{44}\text{Co}_6\text{Mn}_{38}\text{Sb}_{12}$ than in $\text{Ni}_{45}\text{Co}_5\text{Mn}_{38}\text{Sb}_{12}$: the MT shifts with a rate of -2 K/T. The increase of the Co-concentration does not significantly alter the general properties, except for the shift of the MT to lower temperatures, which is accompanied by a marked increase of the magnetization, as previously reported.²⁷

We now turn to the strain studies. The data were taken on both Co-concentrations using the same measuring protocol

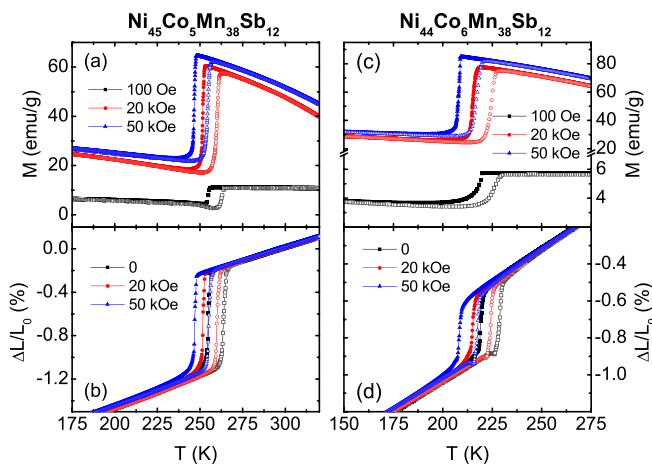


FIG. 1. (a) and (c) Magnetization $M(T)$ and (b) and (d) strain $\Delta L(T)/L_0$ for $\text{Ni}_{45}\text{Co}_5\text{Mn}_{38}\text{Sb}_{12}$ and $\text{Ni}_{44}\text{Co}_6\text{Mn}_{38}\text{Sb}_{12}$, respectively, in different magnetic fields. Solid symbols indicate data obtained upon cooling, while open symbols correspond to data taken upon heating.

TABLE I. Characteristic temperatures of the MT. T_M and T_A correspond to the inflection points in the cooling and heating curves, respectively. The martensitic start and finish temperatures upon cooling, M_s and M_f , and the austenitic start and finish temperatures upon heating, A_s and A_f , are determined from the corresponding onsets in $M(T)$ and $\Delta L(T)/L_0$, respectively.

	T_M (K)	T_A (K)	M_s (K)	M_f (K)	A_s (K)	A_f (K)
$\text{Ni}_{45}\text{Co}_5\text{Mn}_{38}\text{Sb}_{12}$						
magnetization	255.0	263.1	255.8	253.8	261.3	263.9
strain	254.9	264.4	255.6	254.4	262.5	265.4
$\text{Ni}_{44}\text{Co}_6\text{Mn}_{38}\text{Sb}_{12}$						
magnetization	218.7	226.1	220.0	214.9	221.7	229.1
strain	219.2	228.8	220.9	218.6	227.6	230.1

as in the magnetization experiments. Upon cooling in the zero magnetic field, $\text{Ni}_{45}\text{Co}_5\text{Mn}_{38}\text{Sb}_{12}$ exhibits a contraction of $\Delta L_{MT}/L_s \approx -1.0\%$ at the MT. Here, L_s is the length of the sample before the transition. The change in the length is reversible, i.e., the sample recovers its original length after subsequent heating. The shift of the step-like feature toward lower temperatures is in good agreement with the magnetization data (see also Table I). $\text{Ni}_{44}\text{Co}_6\text{Mn}_{38}\text{Sb}_{12}$ exhibits upon cooling a reversible contraction of $\Delta L_{MT}/L_s \approx -0.4\%$ at the MT. For both samples, $\Delta L_{MT}/L_s$ is not sensitive to the application of magnetic fields. This is in contrast to the magnetization data, where the change in magnetization at the MT is strongly enhanced by magnetic field.

In $\text{Ni}_{50-x}\text{Co}_x\text{Mn}_{38}\text{Sb}_{12}$, a reverse MT can be induced by application of a magnetic field.^{11,28} In this series, the field-induced reverse MT can be observed down to liquid helium temperatures.¹¹ However, here we focus on the temperature region close to the thermal MT. Figure 2 presents the magnetization M and strain $\Delta L/L_i$ (L_i is the initial length of the sample before the application of a magnetic field) data at 255 and 258 K for $\text{Ni}_{45}\text{Co}_5\text{Mn}_{38}\text{Sb}_{12}$ as a function of magnetic field. To exclude irreversible effects due to the thermal history, the sample was heated up to 320 K and then cooled down to 100 K before heating to the measuring temperature. The magnetization as well as the change in strain was recorded at constant temperature by sweeping from 0 up to 70 kOe, then to -70 kOe, and back to zero again. This cycle was then followed by a second one.

In the vicinity of the thermal MT, a magnetic field of 7 T is large enough to induce the full magneto-structural transition from the martensitic phase to the austenitic phase in $\text{Ni}_{45}\text{Co}_5\text{Mn}_{38}\text{Sb}_{12}$. The measuring temperatures were chosen in a way that the higher one is $M_s < T < A_s$, i.e., after the initial field sweep, the sample is expected to stay in the austenitic phase. The lower temperature is smaller than M_s . Therefore, all or most of the sample is supposed to convert back to the martensitic phase again upon removing the field. In $\text{Ni}_{45}\text{Co}_5\text{Mn}_{38}\text{Sb}_{12}$, the critical field H_{MT}^{initial} required to induce the MT in the virgin curve is significantly larger than $|H_{MT}|$ in the following field sweep (see Fig. 2(a)), i.e., at 255 K it decreases from $H_{MT}^{\text{initial}} = 47$ kOe to $|H_{MT}| = 42$ kOe. This indicates that at this temperature not the complete austenitic phase converts back to the martensitic phase upon removing the field. The hysteresis in H_{MT} between increasing and decreasing field is large, about 34 kOe at 255 K. After the initial field sweep, we find an almost reversible behavior

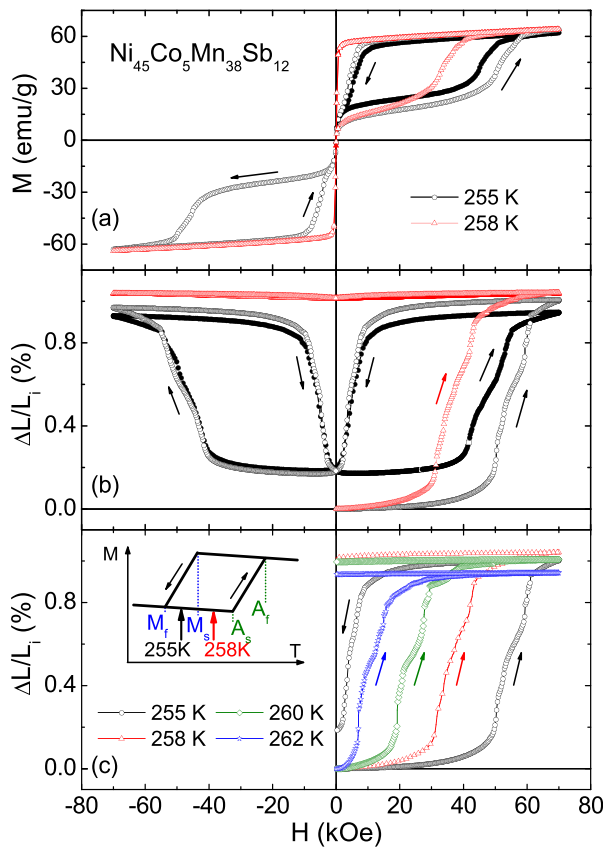


FIG. 2. Magnetization $M(H)$ and strain $\Delta L(H)/L_i$ of $\text{Ni}_{45}\text{Co}_5\text{Mn}_{38}\text{Sb}_{12}$ recorded at constant temperature. L_i is the length of the sample before the application of the magnetic field. (a) and (b) Hysteresis loops of M and $\Delta L/L_i$ at 255 and 258 K. Open and closed symbols indicate the first and second cycles, respectively. (c) $\Delta L(H)/L_i$ at different temperatures between M_f and A_s . The inset illustrates the temperature dependence of the magnetization.

in the $M(H)$ curves. We note that $\text{Ni}_{44}\text{Co}_6\text{Mn}_{38}\text{Sb}_{12}$ behaves similar (not shown).

Strain curves were recorded following the same protocol as used for the magnetization. For $\text{Ni}_{45}\text{Co}_5\text{Mn}_{38}\text{Sb}_{12}$, the results are presented in Fig. 2(b). In addition to the strong variation in magnetization, the field-induced MT also leads to a large change in the length of the sample. At 255 K, $\text{Ni}_{45}\text{Co}_5\text{Mn}_{38}\text{Sb}_{12}$ exhibits a change in the length due to the initial application of a magnetic field of $\Delta L_{MT}^{\text{initial}}/L_i \approx 1.0\%$. A remanent expansion of $\Delta L_{MT}^{\text{m}}/L_i \approx 0.2\%$ remains after the removal of the field. This can be understood since $M_f < 255 \text{ K} < M_s$, and therefore, some part of the sample remains in the austenitic phase. $\Delta L_{MT}^{\text{m}}/L_i$ stays almost constant in the subsequent cycles. As expected, the size of the length change observed in the initial curve is comparable with the value recorded for the temperature controlled MT shown in Fig. 1.

In contrast to the data obtained at 255 K ($T < M_s$), the results at 258 K, a temperature that is in between M_s and A_s (see inset of Fig. 2(c)), display a completely different behavior in magnetostriction as well as in magnetization. The initial application of the magnetic field leads to an expansion due to the reverse MT. However, the length of the sample stays almost constant in the subsequent field sweeps, indicating that the MT does not take place anymore since the sample stays in the austenitic phase. This is in agreement with

the magnetization data taken at the same temperature (see Fig. 2(a)). As shown in Fig. 2(c), upon increasing the temperature further toward A_s , the onset of the length change decreases considerably from about 47 kOe at 255 K to only 6.5 kOe at 262 K, which is about the austenitic starting temperature A_s . We note that at 262 K the change in the length is already slightly reduced, indicating that in the zero magnetic field, already a small part of the sample is in the austenitic phase. We point out that the results for $\text{Ni}_{44}\text{Co}_6\text{Mn}_{38}\text{Sb}_{12}$ are very similar (not shown). The reversible change in strain of around 0.8% is larger than previously reported for other Ni-Mn-based Heusler alloys, such as $\text{Ni}_{50}\text{Mn}_{35}\text{In}_{15}$ with 0.25% (Ref. 37) and $\text{Ni}_{45}\text{Co}_5\text{Mn}_{37}\text{In}_{13}$ with 0.4%.³⁸

The application of uniaxial stress p_u shifts the MT toward higher temperatures and leads to an increase in $\Delta L_{MT}/L_s$ for $\text{Ni}_{45}\text{Co}_5\text{Mn}_{38}\text{Sb}_{12}$ and $\text{Ni}_{44}\text{Co}_6\text{Mn}_{38}\text{Sb}_{12}$. $\Delta L(T)/L_0$ obtained under different uniaxial stresses upon heating and cooling are shown in Fig. 3. We find that the overall shape of the curves does not change due to the application of uniaxial stress. The shift of the MT toward higher temperatures upon increasing p_u is expected, since external (hydrostatic) pressure stabilizes the martensitic phase due to its smaller volume compared with the austenitic phase.^{24,33} After the initial heating run, the samples almost completely recover their initial length upon the subsequent cooling. We note that the width of the MT increases upon increasing p_u . This broadening is mainly caused by a variation in the applied uniaxial stress due to the change in the length of the sample at the transformation.³⁵

Figure 4 displays $\Delta L_{MT}(T)/L_s$ obtained during cooling and heating cycles as a function of the applied uniaxial stress for $\text{Ni}_{45}\text{Co}_5\text{Mn}_{38}\text{Sb}_{12}$ and $\text{Ni}_{44}\text{Co}_6\text{Mn}_{38}\text{Sb}_{12}$. Initially, for

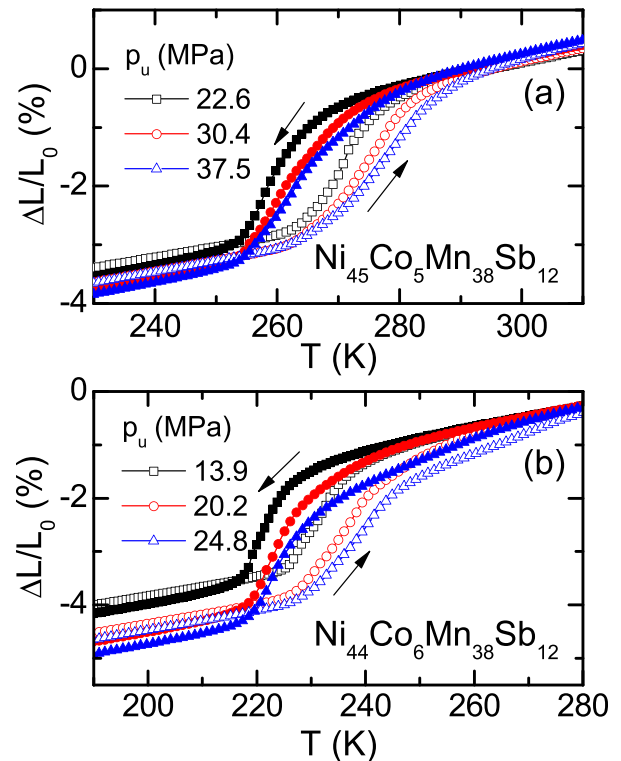


FIG. 3. Strain $\Delta L(T)/L_0$ under uniaxial stress for (a) $\text{Ni}_{45}\text{Co}_5\text{Mn}_{38}\text{Sb}_{12}$ and (b) $\text{Ni}_{44}\text{Co}_6\text{Mn}_{38}\text{Sb}_{12}$. Open and closed symbols indicate data taken upon heating and upon cooling, respectively.

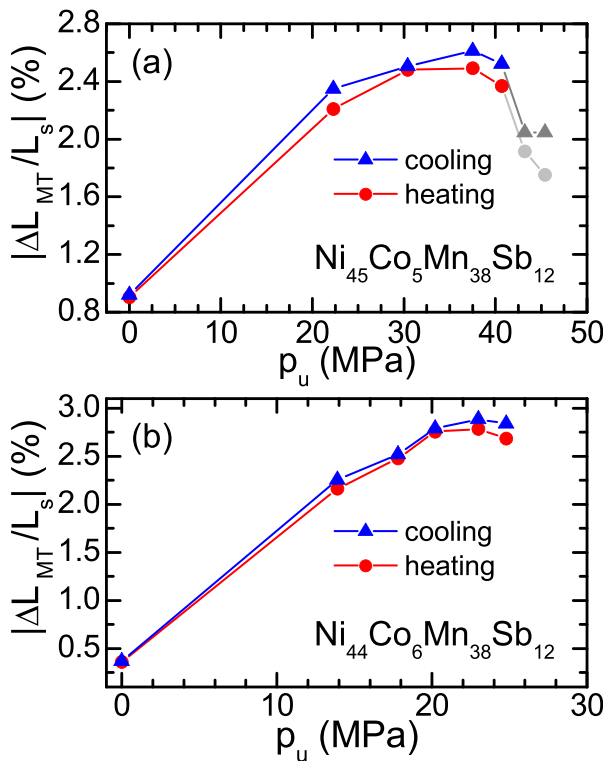


FIG. 4. Relative length change of the sample at the MT $|\Delta L_{MT}/L_s|$ as a function of the applied uniaxial stress p_u for (a) $\text{Ni}_{45}\text{Co}_5\text{Mn}_{38}\text{Sb}_{12}$ and (b) $\text{Ni}_{44}\text{Co}_6\text{Mn}_{38}\text{Sb}_{12}$. L_s is the length of the sample before the MT. Triangles and circles correspond to data recorded upon cooling and upon heating, respectively. The uniaxial stress was applied at room temperature, followed by cooling the sample to 150 K and, after stabilizing the temperature, recording $\Delta L(T)$ upon heating followed by a cooling run.

both investigated materials, $\Delta L_{MT}(p_u)/L_s$ increases almost linearly up to $p_u \approx 20$ MPa. This is mainly caused by a shrinking of the sample in the martensitic phase upon increasing the uniaxial stress (see Fig. 3). Upon increasing the stress further, $\Delta L_{MT}(p_u)/L_s$ displays a trend to saturation. In $\text{Ni}_{45}\text{Co}_5\text{Mn}_{38}\text{Sb}_{12}$, we find an almost constant change in the length of the sample up to 40 MPa, before $\Delta L_{MT}(p_u)/L_s$ suddenly drops. This drop can be related to the formation of cracks in the sample and is not an intrinsic property of the material.

The application of uniaxial stress leads to a significant enhancement of the expansion (contraction) at the MT compared with the unstressed samples by a factor of 1.8 and 7 for $\text{Ni}_{45}\text{Co}_5\text{Mn}_{38}\text{Sb}_{12}$ and $\text{Ni}_{44}\text{Co}_6\text{Mn}_{38}\text{Sb}_{12}$, respectively. Despite this large difference in the magnitude of the enhancement factor, the maximum observed expansion (contraction) is comparable within the experimental uncertainties in both samples.

The previously described findings in $\text{Ni}_{45}\text{Co}_5\text{Mn}_{38}\text{Sb}_{12}$ and $\text{Ni}_{44}\text{Co}_6\text{Mn}_{38}\text{Sb}_{12}$ originate in the strong coupling of structural and magnetic properties present in the Ni-Mn-based Heusler materials. As a consequence, in the vicinity of the MT already small variations in temperature may lead to the observation of either reversible or irreversible behaviors.

The irreversibilities in magnetization and strain data found at temperatures at and below the MT result from a kinetic arrest of the austenitic phase.^{11,28} Upon cooling through the MT, some part of the austenitic phase is retained,

even at temperatures much below the MT. Since the austenitic phase possesses a larger magnetization than the martensitic phase, the magnetization below the MT increases with field due to the presence of the arrested austenitic phase. However, no effect on the strain data $\Delta L(T)/L_0$ is visible in the applied field, i.e., $\Delta L_{MT}/L_s$ does not suffer a significant change in magnetic fields. In the case of an arrested austenitic phase, $\Delta L_{MT}/L_s$ is expected to decrease upon increasing field. This is in contrast to our observations. On the other hand, depending on the orientation of the magnetic field with respect to the different martensitic variants in the sample, the application of a magnetic field can also lead to an increase (or a decrease) in $\Delta L_{MT}/L_s$, i.e., if the direction of the magnetic field coincides with the easy magnetization axis (or not).³⁶ Our results suggest that, in the Ni-Co-Mn-Sb materials, the effect of the austenitic arrest counteracts the alignment of the martensitic variants upon increasing magnetic field.

We now turn to the response to magnetic field at constant temperature. The reverse field-induced MT is completed in our experiments, i.e., the sample transforms from a fully martensitic phase to a fully austenitic phase upon increasing magnetic field, which is accompanied by a pronounced increase in magnetization and strain. The step-like features visible in $\Delta L(H)/L_i$ upon increasing magnetic field might be related to the reorientation of martensitic variants. Upon removing the field again, the magnetization and strain behavior depend sensitively on the measuring temperature. In case the experiment is conducted at a temperature below M_s , the sample recovers almost its initial length. Only for $M_f < T < M_s$, some remanent change in the length $\Delta L_{MT}^{rm}/L_i$ remains, since part of the sample stays in the austenitic phase and a mixed martensitic-austenitic phase is reached at zero field. In contrast to this superelastic or two-way MSM effect, if the experiment is performed at $M_s < T < A_s$, inside the hysteresis region, a one-way MSM effect takes place: the sample stays in the austenitic phase upon removing and applying a negative magnetic field. We have produced a metastable elongation of the material, which can be easily reversed by a small decrease in temperature.

Uniaxial stress can be utilized to further optimize the strain response at the MT. $\Delta L_{MT}/L_s$ is considerably enhanced by the application of uniaxial stress. Despite a large difference in $\Delta L_{MT}/L_s$ at zero stress, $\Delta L_{MT}(p_u)/L_s$ saturates at about the same value for both investigated concentrations. The applied stress breaks the degeneracy associated with the symmetry-allowed martensitic variants.¹⁸ Therefore, increasing uniaxial stress favors the formation of a single martensitic variant. The observed saturation in $\Delta L_{MT}(p_u)/L_s$ suggests that this single variant is established above 20 MPa. In $\text{Ni}_{50-x}\text{Co}_x\text{Mn}_{38}\text{Sb}_{12}$, $x=3$ and 4, no saturation was reported up to 100 MPa, but the observed change in strain is also still below the maximum value in our experiments on $\text{Ni}_{45}\text{Co}_5\text{Mn}_{38}\text{Sb}_{12}$ and $\text{Ni}_{44}\text{Co}_6\text{Mn}_{38}\text{Sb}_{12}$.³³

To conclude, $\text{Ni}_{45}\text{Co}_5\text{Mn}_{38}\text{Sb}_{12}$ and $\text{Ni}_{44}\text{Co}_6\text{Mn}_{38}\text{Sb}_{12}$ display a pronounced step-like change in sample length at their respective temperature and field-induced MT of up to $\Delta L_{MT}^{\text{initial}}/L_0 \approx 1\%$. This value can be strongly enhanced to $\Delta L_{MT}^{\text{initial}}/L_0 \approx 3\%$ by the application of external uniaxial stress, which facilitates the formation of a single martensitic

variant in the material. Thus, $\text{Ni}_{50-x}\text{Co}_x\text{Mn}_{38}\text{Sb}_{12}$, $x = 5$ and 6, are among the Ni-Mn-based MSM alloys the materials with the largest strain response at the MT. In the vicinity of the temperature controlled MT, either a one- or two-way MSM can be generated by the magnetic field depending on small variations in temperature. The metastable length change created by the one-way MSM can be reversed by only a small reduction in temperature bringing the material in the region of the two-way MSM. This behavior, where a slight difference in temperature changes drastically the response of the sample, indicates the large potential these materials have for prospective applications as actuators, sensors, and mechanical switches. The chemical flexibility of the Heusler family further opens the possibility to use elemental substitution, in addition to uniaxial stress and magnetic field, to further optimize the structural and magnetic properties.

This work was financially supported by the ERC Advanced Grant (291472) “Idea Heusler.” R.K. acknowledges support by the German Science Foundation through the Project No. KU 3287/1-1.

- ¹G.-H. Yu, Y.-L. Xu, Z.-H. Liu, H.-M. Qiu, Z.-Y. Zhu, X.-P. Huang, and L.-Q. Pan, *Rare Met.* **34**, 527 (2015).
- ²V. Srivastava, Y. Song, K. Bhatti, and R. D. James, *Adv. Energy Mater.* **1**, 97 (2011).
- ³M. Gueltig, H. Ossmer, M. Ohtsuka, H. Miki, K. Tsuchiya, T. Takagi, and M. Kohl, *Adv. Energy Mater.* **4**, 1400751 (2014).
- ⁴O. Heczko, *Mater. Sci. Technol.* **30**, 1559 (2014).
- ⁵A. Sozinov, N. Lanska, A. Soroka, and W. Zou, *Appl. Phys. Lett.* **102**, 021902 (2013).
- ⁶R. Kainuma, Y. Imano, W. Ito, H. Morito, Y. Sutou, K. Oikawa, A. Fujita, K. Ishida, S. Okamoto, and O. Kitakami, *Appl. Phys. Lett.* **88**, 192513 (2006).
- ⁷K. Ullakko, J. K. Huang, V. V. Kokorin, and R. C. O’Handley, *Scr. Mater.* **36**, 1133 (1997).
- ⁸L. Mañosa, X. Moya, A. Planes, S. Aksoy, M. Acet, E. Wassermann, and T. Krenke, *Mater. Sci. Forum* **583**, 111 (2008).
- ⁹A. Planes, L. Mañosa, and M. Acet, *J. Phys.: Condens. Matter* **21**, 233201 (2009).
- ¹⁰J. Liu, S. Aksoy, N. Scheerbaum, M. Acet, and O. Gutfleisch, *Appl. Phys. Lett.* **95**, 232515 (2009).
- ¹¹A. K. Nayak, C. Salazar Mejía, S. W. D’Souza, S. Chadov, Y. Skourski, C. Felser, and M. Nicklas, *Phys. Rev. B* **90**, 220408(R) (2014).
- ¹²M. Ghorbani Zavareh, C. Salazar Mejía, A. K. Nayak, Y. Skourski, J. Wosnitza, C. Felser, and M. Nicklas, *Appl. Phys. Lett.* **106**, 071904 (2015).
- ¹³C. Salazar Mejía, M. Ghorbani Zavareh, A. K. Nayak, Y. Skourski, J. Wosnitza, C. Felser, and M. Nicklas, *J. Appl. Phys.* **117**, 17E710 (2015).
- ¹⁴T. Krenke, E. Duman, M. Acet, E. F. Wassermann, X. Moya, L. Mañosa, A. Planes, E. Suard, and B. Ouladdiaf, *Phys. Rev. B* **75**, 104414 (2007).
- ¹⁵C. Salazar Mejía, K. Mydeen, P. Naumov, S. A. Medvedev, C. Wang, M. Hanfland, A. K. Nayak, U. Schwarz, C. Felser, and M. Nicklas, *Appl. Phys. Lett.* **108**, 261903 (2016).
- ¹⁶V. K. Sharma, M. K. Chattopadhyay, and S. B. Roy, *J. Phys.: Condens. Matter* **23**, 366001 (2011).
- ¹⁷L. Mañosa, D. Gonzalez-Alonso, A. Planes, E. Bonnot, M. Barrio, J.-L. Tamarit, S. Aksoy, and M. Acet, *Nat. Mater.* **9**, 478 (2010).
- ¹⁸P. O. Castillo-Villa, D. E. Soto-Parra, J. A. Matutes-Aquino, R. A. Ochoa-Gamboa, A. Planes, L. Mañosa, D. Gonzalez-Alonso, M. Stipcich, R. Romero, D. Rios-Jara, and H. Flores-Zuniga, *Phys. Rev. B* **83**, 174109 (2011).
- ¹⁹B. Lu, F. Xiao, A. Yan, and J. Liu, *Appl. Phys. Lett.* **105**, 161905 (2014).
- ²⁰A. K. Pathaka, I. Dubenko, S. Stadler, and N. Ali, *J. Alloy. Compd.* **509**, 1106 (2011).
- ²¹N. V. Rama Rao, M. Manivel Raja, S. Esakki Muthu, S. Arumugam, and S. Pandian, *J. Appl. Phys.* **116**, 223904 (2014).
- ²²J. Liu, T. Gottschall, K. P. Skokov, J. D. Moore, and O. Gutfleisch, *Nat. Mater.* **11**, 620 (2012).
- ²³E. Stern-Taulats, A. Planes, P. Lloveras, M. Barrio, J.-L. Tamarit, S. Pramanick, S. Majumdar, S. Yuce, B. Emre, C. Frontera, and L. Mañosa, *Acta Mater.* **96**, 324 (2015).
- ²⁴A. K. Nayak, K. G. Suresh, A. K. Nigam, A. A. Coelho, and S. Gama, *J. Appl. Phys.* **106**, 053901 (2009).
- ²⁵A. K. Nayak, K. G. Suresh, and A. K. Nigam, *J. Phys. D: Appl. Phys.* **42**, 035009 (2009).
- ²⁶A. K. Nayak, K. G. Suresh, and A. K. Nigam, *J. Phys. D: Appl. Phys.* **42**, 115004 (2009).
- ²⁷A. K. Nayak, K. G. Suresh, and A. K. Nigam, *J. Appl. Phys.* **107**, 09A927 (2010).
- ²⁸A. K. Nayak, K. G. Suresh, and A. K. Nigam, *Appl. Phys. Lett.* **96**, 112503 (2010).
- ²⁹A. K. Nayak, K. G. Suresh, and A. K. Nigam, *J. Appl. Phys.* **108**, 063915 (2010).
- ³⁰A. K. Nayak, K. G. Suresh, and A. K. Nigam, *J. Phys.: Condens. Matter* **23**, 416004 (2011).
- ³¹A. K. Nayak, K. G. Suresh, and A. K. Nigam, *Acta Mater.* **59**, 3304 (2011).
- ³²A. K. Nayak, K. G. Suresh, and A. K. Nigam, *J. Appl. Phys.* **109**, 07A906 (2011).
- ³³R. Millán-Solsona, E. Stern-Taulats, E. Vives, A. Planes, J. Sharma, A. K. Nayak, K. G. Suresh, and L. Mañosa, *Appl. Phys. Lett.* **105**, 241901 (2014).
- ³⁴R. Küchler, T. Bauer, M. Brando, and F. Steglich, *Rev. Sci. Instrum.* **83**, 095102 (2012).
- ³⁵R. Küchler, C. Stingl, and P. Gegenwart, *Rev. Sci. Instrum.* **87**, 073903 (2016).
- ³⁶*Handbook of Magnetic Materials*, edited by M. Acet, L. Mañosa, A. Planes, and K. H. J. Buschow (Elsevier, Amsterdam, 2011), Vol. 19, p. 231.
- ³⁷B. Li, W. J. Ren, Q. Zhang, X. K. Lv, X. G. Liu, H. Meng, J. Li, D. Li, and Z. D. Zhang, *Appl. Phys. Lett.* **95**, 172506 (2009).
- ³⁸Z. Li, C. Jing, H. L. Zhang, D. H. Yu, L. Chen, B. J. Kang, S. X. Cao, and J. C. Zhang, *J. Appl. Phys.* **108**, 113908 (2010).